Near-IR and IR Imaging in Lipid Metabolism and Obesity

Robert G. Buice, Lisa A. Cassis, and Robert A. Lodder*
College of Pharmacy
University of Kentucky Medical Center
Lexington, KY 40536-0082

Abstract

Approximately one-third of Americans are classified as obese. There has long been an interest in drug therapies for obesity. Interest in obesity research and in drug interventions in obesity has greatly increased since the discovery of a protein named leptin, one of apparently many competing biological signals in energy metabolism. The complexity of the obesity problem demands new noninvasive and nondestructive methods for monitoring lipid metabolism and energy expenditure to study the competing biological signals and their effects. A new computer algorithm for spectrometric imaging of living subjects is used to remove artifacts arising from subject motion from spectra and images. The algorithm is sufficiently simple to be implemented easily in hardware for real-time video processing. Because the algorithm can be applied to images, thermogenesis and lipid metabolism in interscapular adipose tissue can be observed directly in unrestrained and unanesthetized subjects using an InSb focal plane array video camera. The accuracy and precision of temperature and spectral measurements are established using laboratory references and prototype drugs in test subjects.

Keywords: image processing, blackbody emission, angiotensin-II, norepinephrine

Abbreviations: near-infrared (near-IR), infrared (IR), tiled Euclidean distances (TED)

Introduction

Approximately one-third of Americans are classified as obese (defined as 20 percent or more over ideal body weight). Americans spend more than $30 billion every year attempting to lose weight. Excessive weight is associated with many health problems, including hypertension, diabetes, heart disease, joint problems, certain types of cancer, and congestive heart failure. Even mild obesity can have adverse consequences. Mildly obese men between ages 35 and 65 have a five-fold greater mortality rate than thinner men of the same ages. The average human male has a higher metabolic rate than the average female, so the average male can consume the same number of calories in food as the average female without gaining weight (or can lose weight at a caloric consumption that would keep the weight of a female constant). There has long been an interest in drug therapies for obesity, in part because this difference in metabolic rates suggests that some chemical means might be safe and effective in control of obesity. However, interest in obesity research and in drug interventions in obesity has greatly increased since the discovery of a protein named leptin (Halaas, 1997).

The leptin protein was first identified in obese mice (mice with a gene named OB that produces a defective protein signal). When researchers injected leptin into the obese mice once a day, it decreased the animals' appetite and increased their metabolic rate. However, most obese humans do not have any problem producing leptin. In fact, most obese people have an overabundance of leptin, producing five times the level found in lean people, on average. The real problem may be that most of the humans with obesity are insensitive to their own leptin.

Drug companies are now pursuing different solutions to the apparent sensitivity problem. One theory is that the problem lies in leptin's target, which may be a receptor in the hypothalamus in the brain. If obesity researchers can figure out what causes the receptor to lose its sensitivity to leptin, they can probably design a drug to counteract the problem.

Nevertheless, while such a drug might be useful as a diet aid, most researchers doubt it could cure obesity. Leptin is likely to be just one of many competing biological signals that tell humans when to eat, what to eat, and how to distribute that food metabolically. Unlike mice, humans also respond to social and psychological influences that affect both eating and exercise behaviors. The complexity of the obesity problem demands new noninvasive and nondestructive methods for monitoring lipid metabolism and energy expenditure to study the competing

biological signals and their effects. Such studies will pave the road to drug therapies for obesity.

Near-infrared (IR) spectrometry has been used in industry for many years to determine lipids (Brennan, 1997). Near-IR spectrometry uses an external light source of many wavelengths to detect sample chemical composition. In contrast, the internal light source provided by blackbody emission is used to determine sample surface temperature. A major advantage of near-IR spectral analysis is its chemical imaging ability. Additionally, near-IR spectral imaging provides information on details of various internal structures including muscle, bone, and arteries (Sevick-Muraca, 1997)(Kang, 1997). Using a specially modified infrared (IR) video camera, different band pass filters permit the measurement of temperature (±0.03ºC) by black body heat emission (IR analysis) or by collection of image spectra over the range of 1000 - 4000 nm (near-IR and IR spectral range). In contrast to near-IR imaging spectrometry, which requires an external light source, infrared imaging is based on internally generated heat radiated as light. Measurements can be made quickly on conscious, freely moving animals placed in a thermoneutral environment.

Near-IR spectra are sometimes subject to extreme baseline variations that arise from the positioning of the sample. When IR or near-IR spectrometric imaging is used for in vivo analysis, artifacts can appear in the images and spectra that from the motions of the living specimen. Variations in sample path length, specular reflectance, and distance to the optics all contribute to the spectral baseline changes (Ham, 1997). Sample motion presents serious problems for near-IR pattern recognition when determining lipid content in the interscapular fat of rats. Laboratory rats, even when restrained or anesthetized, often move at irregular intervals. The motions create peaks and valleys in near-IR spectra and thermal images that are usually corrected individually by a spectroscopist who determines whether the peaks represent real signals.

The averaging of multiple spectra from a sample to reduce noise is a common technique that works well if many spectra are collected and large artifacts exist in only a few of the spectra. Averaging is less effective at reducing noise to acceptable levels when large artifacts are distributed at irregular intervals throughout many of the spectra. Many different filtering schemes are in use (Ham, 1997). In one simple rapid filtering algorithm, three spectra are collected for each sample at n wavelengths. Multiplicative scatter correction is applied to remove additive or multiplicative variations in each spectrum. Each spectrum is then projected as a single point in n-dimensional space (as shown in Figure 1) and the Euclidean distance between each pair of the points is calculated. The two closest spectral points are averaged and the outlier is discarded, resulting in a single spectrum. This filter works well if the sample

moves only once during the series of three scans, however, unrestrained rats move frequently. This filter removes (and in effect, wastes) an entire spectrum if the filter encounters one artifact in the spectrum. The new computer technique used in this study edits localized subspaces of each near-IR spectrum, image, or even spectrometric images for artifacts by tiling Euclidean distances (TED), preserving most of each spectral image even in the presence of artifacts. The increased conservation of spectral information enhances S/N, making the algorithm ideal for the noninvasive study of obesity.

Theoretically, the use of an IR video camera modified to work in the near-IR range should allow for spatially resolved noninvasive measurements of surface temperature (as an index of energy expenditure) and superficial lipid composition (Dempsey, 1997) (as an index of lipid metabolism). The purpose of this study was to decide if near-IR spectrometry and infrared imaging of rats could be used noninvasively to examine regional subcutaneous lipid composition and surface energy expenditure, respectively. In this study, prototype pharmacologic agents with known effects on thermogenesis were administered to rats to demonstrate the effectiveness of near-infrared and infrared techniques. Results from this study show that combined near-IR and IR imaging with a tunable-range video camera detected drug-induced alterations in superficial lipid composition and heat emission.

Materials and Methods

Equipment. Near-IR and IR images were collected using a video camera with a liquid nitrogen-cooled InSb focal plane array detector (Cincinnati Electronics, Mason, OH, USA). Thermal IR imaging was performed using a liquid-nitrogen-cooled InSb focal plane array camera (temperature precision = 0.03º C; 3000 - 5000 nm) with sound annotation capability. No external light source was used in comparing thermogenesis in the different rats, so the intensity of features in the images corresponds to the level of black-body emission from the skin. Temperature calibration was accomplished using a blackbody source closely coupled to a mercury thermometer. Two to four light sources were employed for spectrometric imaging to reduce shadows and achieve the best possible S/N. The sources were 250 W heat lamps with spherical reflectors. Wavelength selection was accomplished using a rugged two-stage system based on a broad bandpass cold filter (77º K) and narrow bandpass near-IR filters mounted in a filter wheel. Full spectra (up to 701 wavelengths) were also collected as needed using a Bran+Luebbe InfraAlyzer 500 with a fiber-optic probe (Bran+Luebbe, Tarrytown, NY, USA). Whenever near-IR cameras were used to collect spectra, two spherical silicon dioxide reflectance standards (one high reflectance and one low reflectance)

were placed in each image to control for variations in light intensity and direction. Images collected on different days and with the light sources in different locations were made comparable by adjusting the gain and offset by multiplicative scatter correction on the images so the intensities on the standards were identical. The specular reflectance on the standards was used to pinpoint the locations of the light sources and to provide a means to calibrate reflected intensity from wet surfaces in tissue samples. Diffuse reflectance from the curved surfaces of the two standards was used to calibrate shaded areas and sloping surfaces in the images. The near-IR and IR images were collected as one second segments of real-time video and saved on computer disk. The near-IR and IR video camera had a frame collection rate of 51.44 frames/sec, making sample target immobilization unnecessary. The TED algorithm was written in Matlab 5.1 (The Math Works, Inc., Natick, MA, USA).

Methods. In its most simple form, the TED technique requires three spectra of images **A**, **B**, and **C**, examined in T tiles of n points each. Where the i^{th} tile is defined by

$$w_i = (1, 2, \ldots, n) + n(i - 1) \mid i \ldots T$$

If TED is used to construct a spectrum from three scans of a sample, then three distances are calculated: dAB, dAC, dBC. The distance calculation is shown for tile T of **A** and **B** in equation 1, where w_j is the j^{th} component of tile w.

$$dAB_{W_i} = \sqrt{\sum_{j=1}^{n} (A_{w_j} - B_{w_j})^2} \quad (1a)$$

$$dBC_{W_i} = \sqrt{\sum_{j=1}^{n} (B_{w_j} - C_{w_j})^2} \quad (1b)$$

$$dAC_{W_i} = \sqrt{\sum_{j=1}^{n} (A_{w_j} - C_{w_j})^2} \quad (1c)$$

The two spectral tiles with the smallest distance between them are then averaged to give the reconstructed tile **R** as shown in equation 2.

$$R_{w_i} = (A_{w_i} + B_{w_i})/2 \mid dAB_{w_i} < dBC_{w_i} \,\&\, dAB_{w_i} < dAC_{w_i} \quad (2a)$$

$$R_{w_i} = (B_{w_i} + C_{w_i})/2 \mid dBC_{w_i} < dAB_{w_i} \,\&\, dBC_{w_i} < dAC_{w_i} \quad (2b)$$

$$R_{w_i} = (A_{w_i} + C_{w_i})/2 \mid dAC_{w_i} < dBC_{w_i} \,\&\, dAC_{w_i} < dAB_{w_i} \quad (2c)$$

Finally the averaged sections are built into a new spectrum **N** as shown by equation 3.

$$N = R_{w_1}, R_{w_2}, \ldots, R_{w_T} \quad (3)$$

The application of the filter to each spectral image allows all artifacts to be removed unless they occur in the same region of a spectral image in two of the three scans. Because an experimental subject is unlikely to move at the same place in each spectrum, TED improves greatly the quality of spectra collected from living subjects. The net effect of TED on a video stream is to make the stream appear a bit more like a slide show and a bit less like a movie. The effect is not too distracting to viewers, but

the point is not to view the video, anyway. TED introduces minor discontinuities in the video stream that the computer can use to decide automatically how many frames can be averaged in groups to increase S/N.

Another algorithm that may provide more fine control of artifact removal is the forward running Euclidean distance (FRED) algorithm. FRED reconstructs spectra/images in a similar way to TED, except that the calculations are done on a window of points that slides along the spectral images, replacing only the point in the center of each window, based on the values of the center point and a defined neighborhood of adjacent points. The window advances in one wavelength increments, while TED advances in increments of an entire tile of wavelengths.

Tests. Two types of imaging studies were performed. The first study was conducted to determine the accuracy and precision of surface temperature measurements made by a near-IR video camera on a simple hand-held moving target (a laboratory thermometer). Ambient lighting was permitted to vary in intensity and direction during this study to simulate the following of a freely moving, living target with the camera. Thermal IR emission was also determined in joules per second (watts) using standard software based upon Stefan's Law. A proprietary drug known to increase metabolic rate and cause weight loss was then administered to experimental obese subjects once each day for two weeks. Control obese subjects received a dose of phosphate buffered saline. Spatially resolved temperature measurements were made on these subjects to learn whether the increase in metabolic rates could be detected by remote IR emission imaging.

The second study demonstrated the accuracy and precision of chemical composition measurements made with a near-IR video camera from a distance of one meter in a diffuse reflectance mode. Ten mixtures of sucrose in a sodium chloride matrix were prepared for this study. The light and dark ceramic optical reflectance standards were placed beside 0.1 g samples of these mixtures during near-IR imaging. Subsequently, absorbance of the pair of lipid peaks between 1700 and 1800 nm was monitored in rats shaved over their interscapular fat pad as the rats were administered norepinephrine (400 μg/kg, s.c., a compound known to mobilize lipids), angiotensin II (200 μg/kg, s.c., a compound implicated in lipid metabolism), or phosphate buffered saline. The pair of optical reflectance standards was present again in every frame collected to enable image corrections to be made. Spatially resolved spectrometric measurements were made on these subjects to learn whether changes in subcutaneous lipid composition could be detected by near-IR diffuse reflectance spectrometry *in vivo*.

Results and Discussion

Figures 2a and 2b show consecutive frames from real-time IR video imaging of an ambulatory rat. In regular use, colors are employed to represent temperature in spectral order, with violet indicating the lowest temperature and red indicating the highest temperature. However, for publication in this figure, the colors have been converted to gray-scale. Note that in Figure 2a the leg in the inset box shows a high temperature that appears as a dark zone. Figure 2b shows that the rat has moved his right foreleg (enclosed in the black box in the figures). Averaging the three frames around Figure 2a produces Figure 2c, in which the leg is lighter than in Figure 2a (i.e., an incorrect temperature measurement).

Figure 2d shows the thermal image of an ambulatory rat reconstructed from three partial images using the TED algorithm. The image artifacts due to movement have been removed (the leg now appears in the proper color, red) and heat from the interscapular fat (ISF) pad is clearly visible (red represents the hottest portion of the image). Increasing thermogenesis in the subcutaneous ISF raises the temperature of the skin that covers the pad, making the ISF visible in the image.

Figure 3a shows the hand-held laboratory thermometer (at 32 ° C in the image) used to determine the accuracy and precision of surface temperature measurements made by a near-IR video camera on a moving target with specular and diffuse reflectance noise. Temperature measurements were made by imaging the thermometer bulb, marked by the inset white box in Figure 3a. The thermometer was heated to equilibrium at 50 ° C and allowed to cool as it moved in front of the camera. Temperature calibrations were made with and without TED filtering of the images. The calibration results appear in Table I, and the results show that infrared imaging is an effective means of determining surface temperatures even on moving targets. The TED algorithm does not appear to improve the calibration itself, but instead improves the performance of the calibration on cross validation (prediction of sample surface temperatures on images not used to create the calibration). The improvement of cross validation is not surprising because the sample motion (which is removed by TED) is the only factor that varies on replicate trials of the moving target experiment.

Radiated power of the thermometer bulb was calculated with TED using the camera and software as the bulb cooled from 50 to 21 ° C (see Figure 3b). Radiated power is governed by Stefan's Law: $P_{net}=Ae(T^4-T_o^4)$, where P_{net} is power output in J/sec (watts), $= 5.6696\text{x}10^{-8}$ W $m^{-2}K^{-4}$, and e is emissivity (approx. 0.9 for skin).

Having established the ability of IR imaging and the TED algorithm to determine surface temperatures of moving targets in uneven illumination, infrared emission imaging was tested in the monitoring of relative metabolic rates. A proprietary drug known to increase metabolic rate and cause weight loss was administered to experimental genetically obese subjects once each day for two weeks. Control obese subjects received a dose of phosphate buffered saline. Spatially resolved temperature measurements were made on these freely moving subjects to learn whether the increase in metabolic rates could be detected by remote IR emission imaging. Figure 4a is the thermal image of saline-treated obese subject. The tail and feet are barely visible because the surface temperatures of these appendages are at nearly ambient temperature. Figure 4b is the thermal image of a drug-treated obese subject. Increased metabolic rate in this subject led to an increase in the surface temperature of many body regions (the tail, especially, serves as a thermoregulatory organ in these subjects), rendering these regions clearly visible in the image. In Figure 4c, surface temperatures of different body zones in drug-treated and control obese subjects are shown. All temperature differences marked on Figure 4c with an asterisk were significant at $p<0.05$. A t-test was used on temperature data from each zone to establish significance, with n=20 measurements for ISF, n=10 measurements for tail, n=5 measurements for eyes, n=20 measurements for dorsal area over abdomen, and n=10 measurements for feet. The number of measurements obtained for each zone is figured by the relative difficulty in obtaining different independent views of the zones in freely moving subjects. The height of the bars marks the mean temperature of each zone. The error bars shown depict one SD. The data show that the drug-induced increase in metabolic rates could be determined by remote IR emission imaging.

The accuracy and precision of chemical measurements using the near-IR cameras were initially determined using 100 mg standards composed of varying amounts of sodium chloride and sucrose. Due to variations in positioning of the light sources and detector drift, a light and dark spherical SiO_2 reflectance standard (at the rear in Fig. 5a) were used to correct gain and offset of sample images at each wavelength. Using the reflectance measurements obtained at several different wavelengths, the near-IR camera could quantify sucrose in the samples with an SEE=1.2% and SEP=1.3% over the range of concentrations (0-100%) in prepared standards (n_c=10, n_v=8 samples) (see Fig. 5b). Using a reference ceramic disk to measure noise levels and two 150W tungsten lamps as a light source, the measured noise level on a single near-IR camera image was determined to be 200 microabsorbance units (ref 0 O.D.) in a 7-sec scan containing 256 frames. This level of noise is at the lower limit of what can be measured with the analog-to-digital converter (A/D) reading the camera's focal plane array. These data show changes in chemical composition can be detected by near-IR diffuse reflectance spectrometry using a near-IR video camera from a distance of one meter in a diffuse reflectance mode.

Near-IR spectra of subcutaneous interscapular fat were obtained from norepinephrine-treated rats (n=8) (see Figure 6a). Absorbances at two major lipid peaks between 1700 and 1800 nm were monitored over time after injection. Spectra were pretreated with multiplicative scatter correction and reconstructed from inverse principal axis transformation using the principal axis loadings that correlated to elapsed time. Lipid mobilization in the ISF appears as a steady loss of both peak areas with the passage of time. Near-IR spectra of subcutaneous interscapular fat were also obtained in angiotensin-II-treated rats (n=8) (see Figure 6b). Angiotensin-II appears to cause selective mobilization of lipids, first drawing down lipids with the high energy C-H stretch overtone, and later lipids with the lower energy overtone at 1760 nm. The data show that spatially resolved spectrometric measurements made *in vivo* can determine changes in subcutaneous lipid composition.

Conclusion

The TED technique for spectral and image filtering removes artifacts from a set of spectra much faster than manual editing (in seconds instead of hours or days). The resulting spectrum or image is unbiased by the leverage of artifact peaks encountered in spectral averaging, eliminating "ghosts" and "smears" that appear in averaged images at reduced intensity. This new algorithm also enables the monitoring of lipid metabolism and thermogenesis in the interscapular fat pads of rats with a modern near-IR/IR video camera.

These data show that accurate and precise remote measurement of surface temperature in moving subjects is possible with the TED algorithm. In addition, drug-induced increases in metabolic rates can be detected by remote IR photon-emission imaging. Accurate and precise chemical composition measurement is also possible using a remote near-IR camera with a tunable light source and light and dark reflectance standards in each captured frame. Drug-induced changes in lipid composition can be detected in subcutaneous interscapular fat pads by near-IR spectrometry.

The use of image correction in near-IR spectrometric imaging also allows near-IR to be employed in places where sterility must be preserved (e.g., the spectra may be obtained from a distance). TED image correction permits analysis when the samples are subject to motion, such as in the near-IR analysis of carotid plaques during surgery, or in the monitoring of sterile pharmaceuticals during the manufacturing and packaging process.

Acknowledgement

This research was supported in part by the National Science Foundation through grant number CHE 9257998 and by the University of Kentucky Medical Center Research Fund.

References

Brennan JF 3rd, Romer TJ, Lees RS, Tercyak AM, Kramer JR Jr, Feld MS, Determination of human coronary artery composition by Raman spectroscopy. Circulation 96(1), 99-105 (1997)

Dempsey RJ, Cassis LA, Davis DG, Lodder RA, Near infrared imaging and spectroscopy in stroke research: Lipoprotein distributions and disease, Ann. NY Acad. Sci., 820:149-169, (1997)

Halaas JL, Boozer C, Blair-West J, Fidahusein N, Denton DA, Friedman JM, Physiological response to long-term peripheral and central leptin infusion in lean and obese mice. Proc Natl Acad Sci U S A 94(16), 8878-8883 (1997)

Ham FM, Kostanic IN, Cohen GM, Gooch BR, Determination of glucose concentrations in an aqueous matrix from NIR spectra using optimal time-domain filtering and partial least-squares regression. IEEE Trans Biomed Eng 44(6), 475-485 (1997)

Kang KA, Bruley DF, Chance B, Feasibility study of a single- and multiple-source near-infrared phase-modulation device for characterizing biologic systems. Biomed Instrum Technol 31(4), 373-386 (1997)

Sevick-Muraca EM, Lopez G, Reynolds JS, Troy TL, Hutchinson CL, Fluorescence and absorption contrast mechanisms for biomedical optical imaging using frequency-domain techniques. Photochem Photobiol 66(1), 55-64 (1997)

Figures

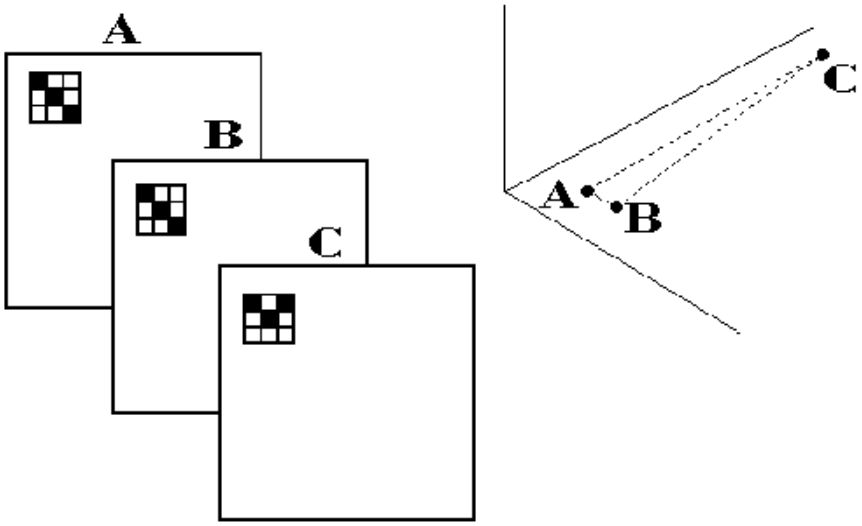

Figure 1. Diagram illustrating how the TED algorithm detects spectral and image artifacts by calculating Euclidean distances. In this example, the point **C** will be excluded and the new multidimensional data point will be the mean of **A** and **B**.

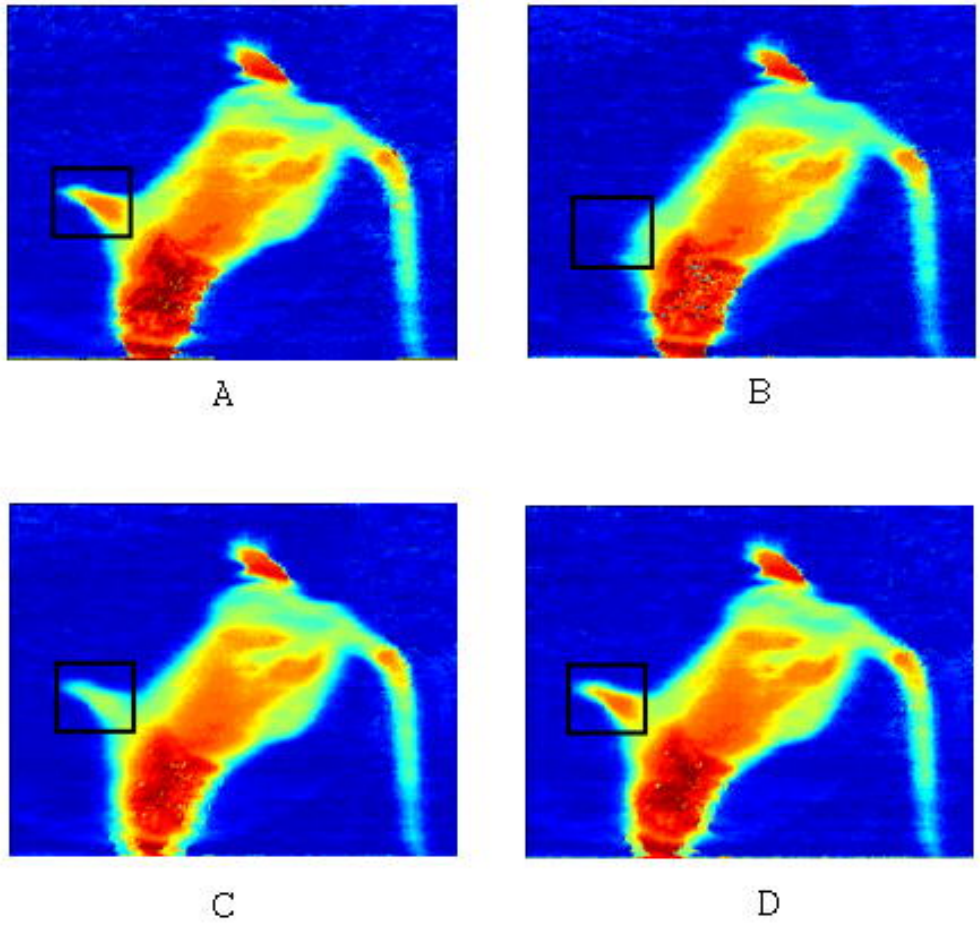

Figure 2a. A frame captured from real-time thermal image video. Colors are used to represent temperature in spectral order, with violet indicating the lowest temperature and red indicating the highest temperature. Note the relatively high temperature (denoted by the red color) of the leg marked by the inset square.
b. One consecutive frame past the image in figure 2a. The leg has been moved by the rat and is no longer visible.
c. A reconstructed thermal image of the rat by averaging the frames around Fig. 2a. Note that the apparent temperature of the foreleg in the box is lower than same leg in Fig. 2a, (The incorrect measurement of temperature appears green rather than red in the thermal color code).
d. A reconstructed thermal image of the rat using the TED algorithm on the frames around Fig. 2a. Notice that the temperature of the foreleg (shown in red) is now in agreement with Fig. 2a.

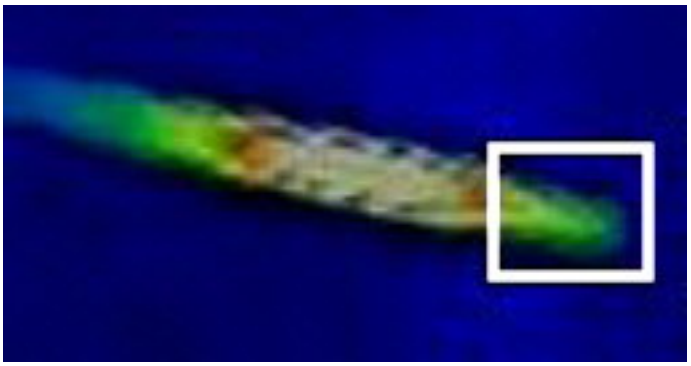

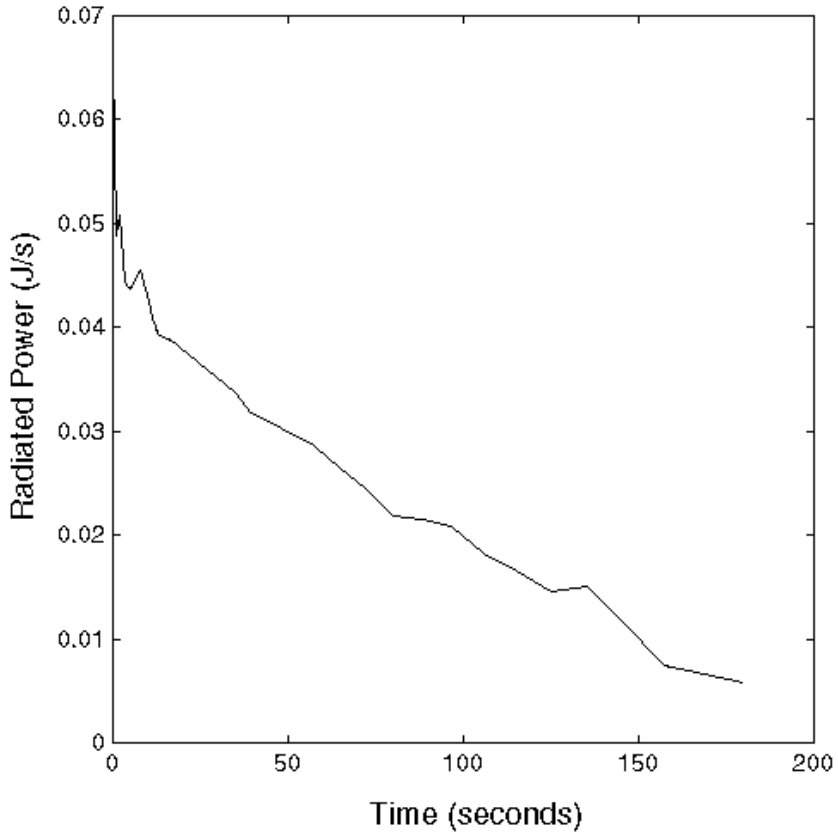

Figure 3a. (top) Thermal IR image of a hand-held thermometer at 32 ° C. A temperature calibration was made on a hand-held thermometer to demonstrate the effect of small sample motions on temperature measurement by IR imaging. Temperature measurements were made on the thermometer bulb, marked by the inset white box. The thermometer was heated to equilibrium at 50 ° C and allowed to cool as it moved in front of the camera. Temperature calibrations were made with and without TED filtering of the images.
b. (bottom) Radiated power of the thermometer bulb calculated using the camera and software as the bulb cooled from 50 to 21 ° C.

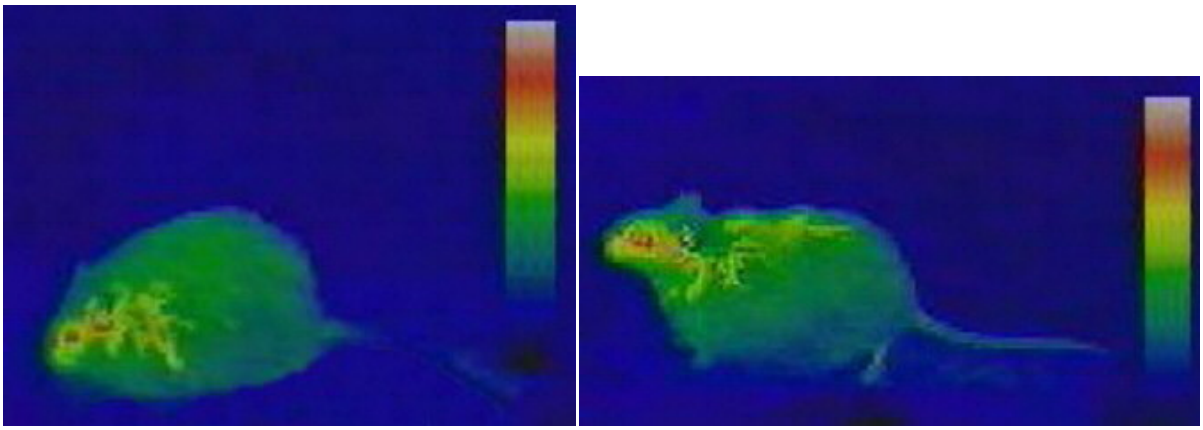

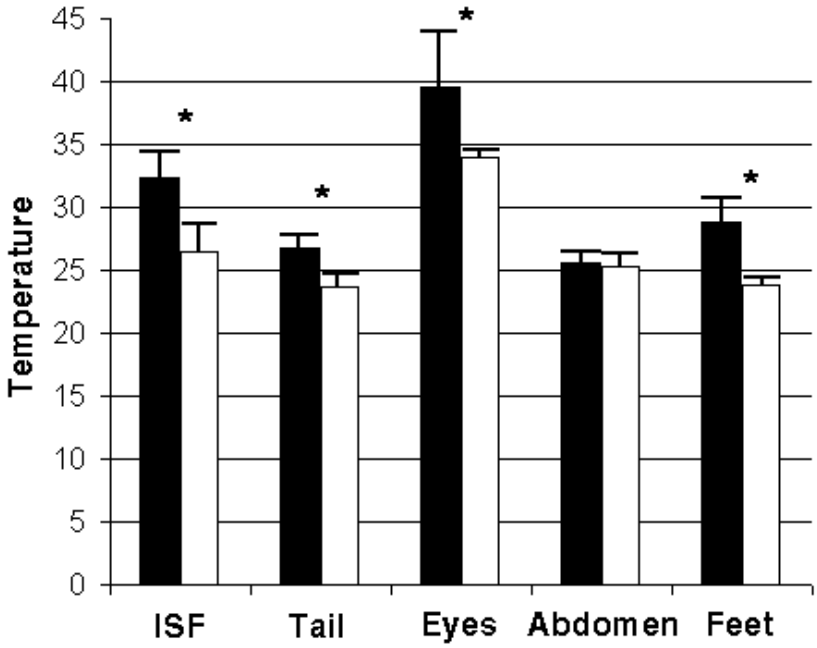

Figure 4a. (top, left) Thermal image of saline-treated obese subject. The color bar at right is used to help adjust the camera to display a full range of intensities from each selected body region.
b. (top, right) Thermal image of drug-treated obese subject.
c. (bottom) Surface temperatures of different body zones in drug-treated and control obese subjects. All temperature differences marked with an asterisk were significant at $p<0.05$. N=20 measurements for ISF, n=10 for tail, n=5 for eyes, n=20 for dorsal area over abdomen, and n=10 for feet. The height of the bars marks the mean temperature of each zone. The error bars are one SD.

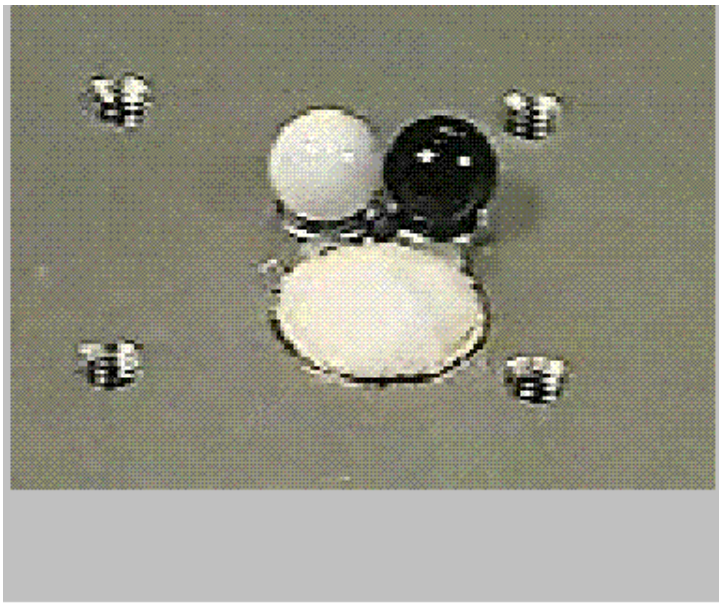

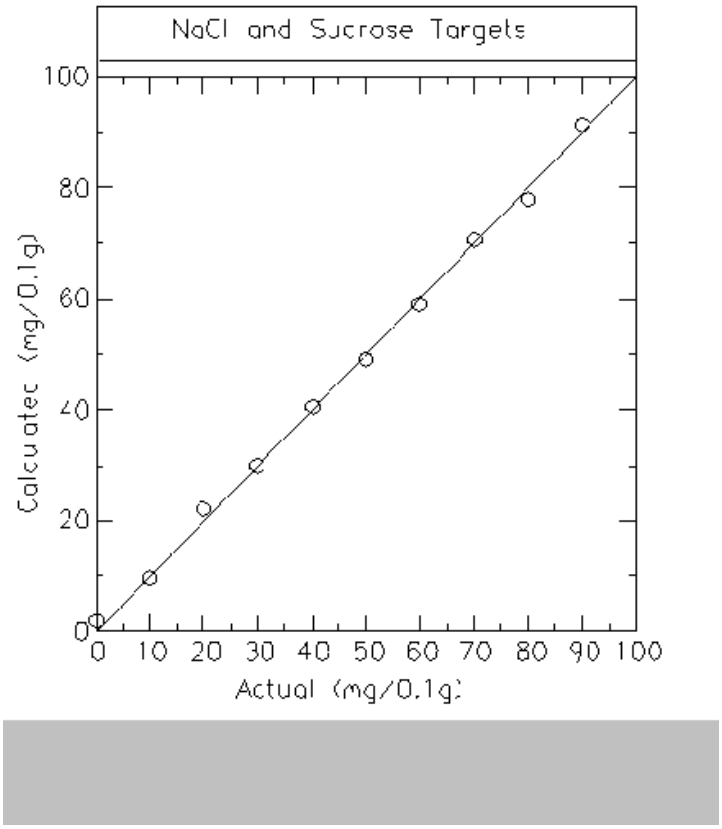

Figure 5a. (top) Near-IR diffuse-reflectance spectrometric imaging of sodium chloride/sucrose mixtures on an optical table. The light and dark optical reflectance standards are at the rear of the image, while the sodium chloride/sucrose mixtures were placed in the front.
b. (bottom) Calibration performance for the near-IR diffuse-reflectance spectrometric imaging of sodium chloride/sucrose mixtures. $r^2 = 0.99$, SEE=1.2% and SEP=1.3%.

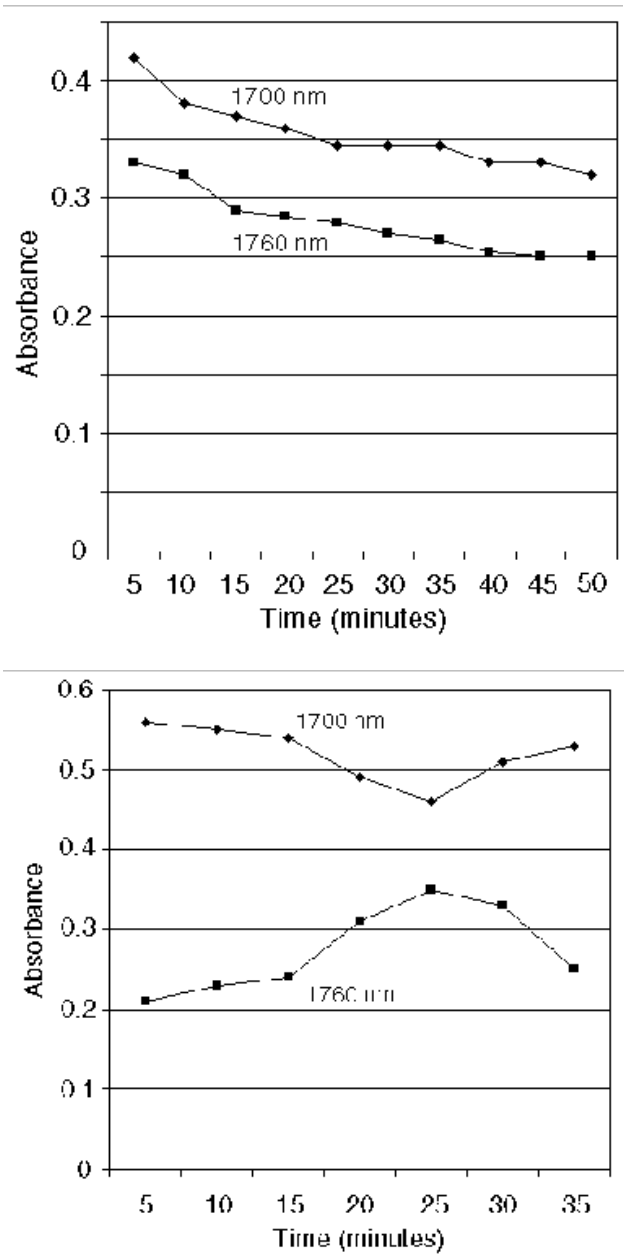

Figure 6a. Near-IR spectra of subcutaneous interscapular fat in norepinephrine-treated (n=8) rats. Absorbances at two major lipid peaks between 1700 and 1800 nm were monitored over time after injection. Spectra were pre-treated with multiplicative scatter correction and reconstructed from inverse principal axis transformation using the principal axis loadings that correlated to elapsed time. Lipid mobilization in the ISF appears as a steady loss of both peak areas with the passage of time.
b. Near-IR spectra of subcutaneous interscapular fat in angiotensin-II-treated rats (n=8). Angiotensin-II appears to cause selective mobilization of lipids, first drawing down lipids with the high energy C-H stretch overtone, and later the lower energy overtone at 1760 nm.

Table I. Surface Temperature Measurement on a Moving Thermometer Bulb (n_c=30 images, n_v=28 images)

	r^2	SEE	SEP	F-test $p<0.05$
TED	0.99	1.0 ° C	1.8 ° C	significant
No TED	0.99	0.9 ° C	3.3 ° C	not significant